ISSN 0915-633X

NATIONAL INSTITUTE FOR FUSION SCIENCE

Long Time Scale Evolution of Collisionless Driven Reconnection in a Two-Dimensional Open System

W. Pei, R. Horiuchi and T. Sato

(Received - Apr. 9, 2001)

NIFS-693 Apr. 2001

RESEARCH REPORT
NIFS Series

TOKI, JAPAN

Long Time Scale Evolution of Collisionless Driven Reconnection in a Two-Dimensional Open System

Wenbing Pei[a], Ritoku Horiuchi[a b], and Tetsuya Sato[a b]
[a] *The Graduate University for Advanced Studies*
[b] *Theory and Computer Simulation Center, National Institute for Fusion Science*
Toki, 509-5292, Japan

abstract

Long time scale evolution of collisionless driven reconnection in an open system is investigated by means of two-dimensional full particle simulation based on an open boundary model. Collisionless reconnection is externally driven by the plasma inflow, which is mainly controlled by two key parameters of an external driving electric field, i.e., the strength E_0 and the early non-uniformity scale x_d. The strength E_0 controls reconnection rate, while the scale x_d controls the current layer shape and thus the magnetic field configuration. It is found that the dynamical behavior of collisionless reconnection is sensitive to x_d and less to E_0 in our simulation parameter range. In the small x_d case, the system evolves toward a steady state in which the reconnection rate is balanced with the external driving field E_0. As x_d increases, the reconnection evolution exhibits an intermittent phenomenon because of the frequent excitation of magnetic islands near the original X point.

KEYWORDS collisionless driven reconnection, two-dimensional open system, particle simulation, steady reconnection, intermittent reconnection phenomenon

I INTRODUCTION

Collisionless magnetic reconnection is recognized as a fundamental process both in space plasmas[1-3] and in laboratory plasmas[4-7] by allowing magnetic energy conversion into plasma energy and plasma transport. Magnetic reconnection requires the existence of a dissipation mechanism which is responsible for breaking the frozen-in constraint by inducing an electric field in a field reversal region called dissipation region. In a two-dimensional (2D) collisionless plasma, dissipation mechanism is generally thought to be provided by microscale particle kinetic effects, i.e., the inertia effect[2,8,9] and the thermal effect[2,10-14] based on the nongyrotropic (meandering) motion. It is clear that the evolution of collisionless reconnection is controlled by the particle kinetic effects.

Magnetic reconnection is often divided into spontaneous reconnection and driven reconnection. Spontaneous reconnection occurs due to internal instabilities such as the collisionless tearing instability[1,3,5,14-19]. Driven reconnection[10,11,20-25] refers to an open system where plasma inflow and magnetic field are supplied from upstream boundaries. In fact, although magnetic reconnection is a localized process, it gives rise to large-scale plasma transport. In this sense even for spontaneous reconnection its evolution is easily affected by external other physical processes. Thus the realistic system is generally open. In addition a driven system may be regarded as a section of whole reconnection system so as to keep higher spatial resolution of the dissipation region with microscopic scales under the condition of the limited computer resource.

The particle simulations of collisionless driven reconnection were performed by Horiuchi and Sato[10,11]. They found that the evolution of collisionless reconnection is controlled not only by the internal microscopic processes such as electron dynamics and ion dynamics, but also by the external driving condition. However, their studies are limited to an early ramp-up phase because a periodic condition is used at the downstream boundary.

The purpose of the present work is to explore long time scale evolution of collisionless driven reconnection by extending the previous model[11] to an open kinetic model with free conditions at the downstream boundaries. Especially, we discuss whether steady reconnection is realized for an open system with a constant energy supply. Although the steady state is certainly a possible tendency of evolution, it is not always realized even if there exists a steady state in mathematics. For example, Kitabata *et al.*[25] and Amo *et al*[26] have demonstrated intermittent phenomena in the magnetic reconnection processes by using magnetohydrodynamics simulation. There are two factors that disrupt the steady state. One comes from the disparity of internal physical process and external physical condition. The steady reconnection is realized when the reconnection rate is balanced with the external driving flow rate. That is, the internal

processes (electron dynamics and ion dynamics) should adjust themselves to accommodate the external driving condition, because magnetic reconnection is controlled by both the internal microscopic process and the external driving condition. However, the adjustment is limited. Beyond this limit, there is no steady state. The other is due to an instability even for the case in which there exists a steady state. If such a steady state itself is unstable due to some instabilities such as the tearing instability, or if an instability can be excited in the process of system evolution, the reconnection can hardly tend toward this steady state, but often behaves intermittent. Thus the evolution of collisionless driven reconnection depends closely on the rate and spatial pattern of driving flow. In this paper we will clarify the mechanism of collisionless driven reconnection, and focus on the effect of the driving conditions on the long time scale evolution of driven reconnection such as tending to a steady state or exhibiting an intermittent phenomenon.

II SIMULATION MODEL

We have developed a two-and-half dimensional explicit electromagnetic particle simulation code for an open system based on the previous version[11]. The simulation is performed in the x-y plane. At the upstream boundary ($y = \pm y_b$) the plasma inflow is driven by an external electric field imposed in the opposite z direction. The remaining components are taken as $E_x = 0$ and $\partial_y E_y = 0$. The downstream boundary ($x = \pm x_b$) is free, across which plasma can freely flow in or out. Thus, the total particle number in the system changes with time, but the charge neutrality condition is always satisfied. The downstream boundary conditions for field quantities are assumed that E_x, E_y and $\partial_x E_z$ are continuous. As to the boundary condition for particles, the net number of particles passing the boundary during one time step is determined by calculating the plasma outflow, and thereby some particles are re-inputed.

The initial condition is given by a Harris-type equilibrium as

$$\begin{aligned} B_x(y) &= B_0 \tanh(\mathrm{y/L}), \\ P(y) &= (B_0^2/8\pi)\mathrm{sech}^2(\mathrm{y/L}), \end{aligned} \tag{1}$$

where B_0 is a constant and L is the scale height along the y-axis. The magnetically neutral sheet is on the x-axis (y=0). The initial particle distribution is a shifted Maxwellian with a spatially constant temperature ($T_e = T_i$) and the average particle velocity which is equal to the diamagnetic drift velocity.

The simulation is carried out on a 512×128 point grid by using 6.4 million particles. The aspect ratio of simulation box is chosen as $x_b/y_b = 6$. The main parameters are in the following: the mass ratio of ion to electron $m_i/m_e = 25$, $\omega_{pe0}/\omega_{ce0} = 3.5$, $L = 0.8y_b \approx 3\rho_{i0}$, where ω_{pe0} is the plasma frequency, ω_{ce0} is the electron cyclotron frequency associated with B_0, and ρ_{i0} is the ion Larmor radius. The relations $L > \rho_{i0} > c/\omega_{pe0} > \Delta y$ hold in the initial configuration. The time step is chosen as $\omega_{ce0}\Delta t = 0.02$.

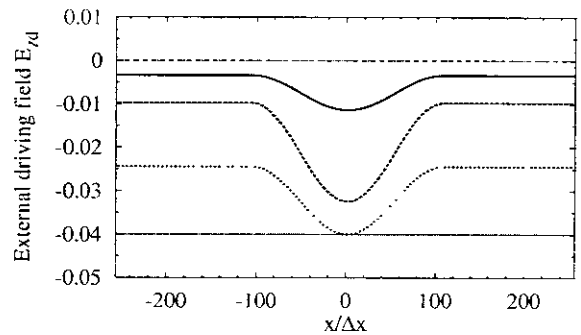

Figure 1: The spatial profiles of the external driving electric field at the input boundary at the times $\omega_{ce0}t = 0, 10.2, 20.4, 81.6$ and 143 for the case of $E_0 = -0.04B_0$ and $x_d/x_b = 0.42$.

The external driving electric field $E_{zd}(x,t)$ imposed at the upstream boundary at five different times, i.e., $\omega_{ce0}t = 0$, 10.2, 20.4, 81.6 and 143, is shown in Fig. 1. After $\omega_{ce0}t = 143$, E_{zd} keeps a constant E_0 which is a necessary condition for steady reconnection. Another important parameter characterizing E_{zd} is the early-phase non-uniformity scale x_d. It is worthwhile to note that although E_{zd} is uniform in the later time, the corresponding magnetic field is always non-uniform, depends strongly on x_d and can change with time. According to the Faraday law the y-component of magnetic field at the input boundary, B_{yd}, has the form ($\omega_{ce0}t > 143$) as

$$\begin{aligned} B_{yd}(x,t) &\propto (E_0/x_d)\sin(\phi(x)), \\ \phi(x) &= \begin{cases} -\pi, & x < -x_d \\ \pi x/x_d, & -x_d \le x \le x_d \\ \pi, & x > x_d. \end{cases} \end{aligned} \tag{2}$$

The function form $\sin(\phi(x))$ in the above expression comes from the fact that $E_{zd}(x,t) \propto \cos(\phi(x))$ for $\omega_{ce0}t < 143$. Correspondingly, $\partial_y B_{xd} \approx \partial_x B_{yd}$ where the current is approximately zero. This means that B_{xd} is not fixed but related to inner field structure. In other words, the internal reconnection process can adjust the boundary magnetic field, too. In fact, the non-uniformity scale x_d affects the curvature radius of magnetic field lines

at the input boundary, and thus the divergency of plasma inflow. In order to study the dependence of the reconnection process on the profile of driving electric field, we perform simulation runs with various sets of E_0 and x_d/x_b listed in Table I.

TABLE I. Simulation parameters

Run	E_0/B_0	x_d/x_b	Tendency
1	-0.04	0.42	steady
2	-0.04	0.62	steady
3	-0.04	0.83	intermittent
4	-0.06	0.42	steady
5	-0.06	0.62	steady
6	-0.06	0.83	intermittent
7	-0.08	0.42	steady
8	-0.08	0.62	steady
9	-0.08	0.83	intermittent

III SIMULATION RESULT

Table I shows the simulation parameters for nine runs and the corresponding temporal behavior of magnetic reconnection. The steady reconnection is realized for all of runs of $x_d/x_b \leq 0.62$. The intermittent phenomena can take place in three cases of $x_d/x_b = 0.83$. It is evident that the evolving way of reconnection is insensitive to E_0. First we will examine some features of steady magnetic reconnection mainly based on the result of Run 1.

Steady reconnection

Figure 2 shows the temporal evolutions of the reconnection electric field E_r for Runs 1, 4 and 7 with $x_d = 0.42$, where the thin dotted lines stand for the values of the external driving electric field E_0. The reconnection electric field is defined as the out-of-plane electric field at the main X point if there are more than one X point, which is a direct measure of the reconnection rate. There exist two temporal phases in the evolution of the reconnection electric field, i.e., growing phase and saturation phase. The reconnection field experiences a fast growth, starts to saturate and then gradually approaches the external driving field E_0 though the fluctration amplitude increases with E_0. These results lead us to conclusion that the system transits to a steady reconnection state in which the reconnection rate E_r is balanced with the flux input rate E_0 at the boundary. This conclusion is consistent with the requirement for a steady state. For 2D steady reconnection the out-of-plane electric field becomes uniform in space and constant in time, and therefore this field must be equal to the external driving field E_0 at the boundary, which is verified from Faraday's law.

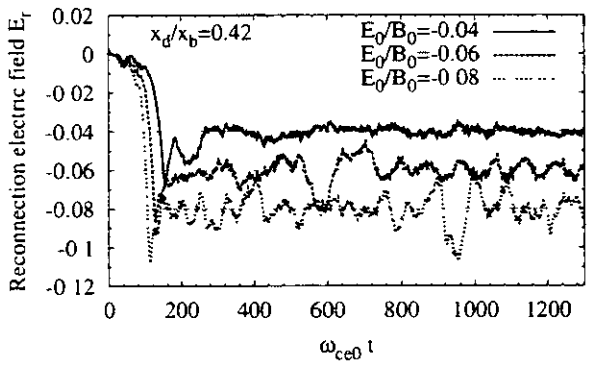

Figure 2: The temporal evolutions of reconnection electric field E_r for Runs 1, 4 and 7.

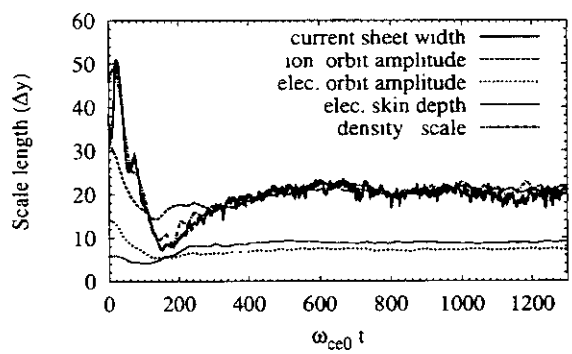

Figure 3: The temporal evolutions of five spatial scales, i.e., the half-width of current layer d_{jz}, the electron Larmor radius ρ_e, the ion Larmor radius ρ_i, the electron skin depth δ_e $(= c/\omega_{pe})$, and ion density scale d_h, where the scales are calculated from the profiles in the y direction passing the X point and are normalized by Δy.

Figure 3 shows the temporal evolutions of five spatial scales where the scales are calculated from the profiles in the y direction passing the X point and are normalized by Δy. The five curves represent half-width of current layer d_{jz}, ion Larmor radius ρ_i, electron Larmor radius ρ_e, electron skin depth δ_e $(= c/\omega_{pe})$, and ion density scale d_h, respectively. Here, the Larmor radius ρ_s of species s is defined at a position $y = y_s$ where the local Larmor radius $\rho_s(y)$ satisfies the condition $\rho_s(y_s) = y_s$. If B_x is a linear function of y, $\rho_s(y_s)$ is equivalent to the meandering orbit amplitude used in the previous papers[10,11]. The density scale d_h is defined as the half-width in the case of single-peak profile of density or the half peak-to-peak distance

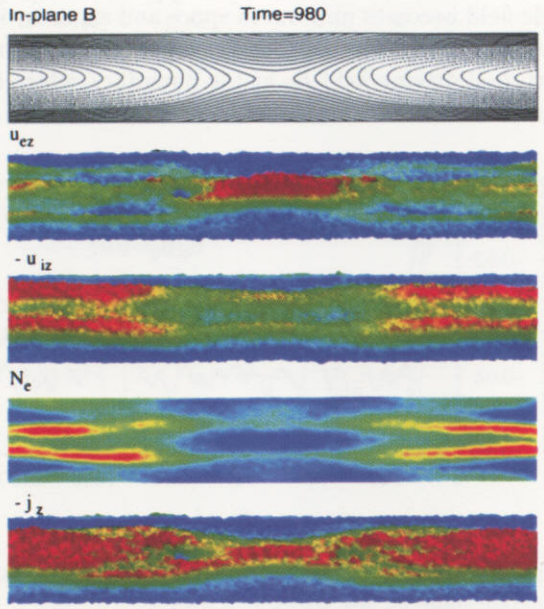

Figure 4: The spatial structures of the in-plane magnetic field, the out-of-plane velocities of electron flow u_{ez} and ion flow $-u_{iz}$, the electron number density N_e and the out-of-plane current density $-j_z$ where u_{ez}, $-u_{iz}$ and $-j_z$ are perspectively plotted.

in the case of two-peak profile. When the current layer is compressed close to the electron scale δ_e or ρ_e, the reconnection field starts to saturate. As time goes on, however, d_{jz} gradually relaxes to ρ_i again and the reconnection proceeds with a constant rate. Figure 3 also demonstrates another two features: (1) both d_{jz} and d_h almost change with the same rate at all times, and approach ρ_i after the reconnection rate reaches maximum; and (2) δ_e is slightly wider than ρ_e in the saturation phase. These features are most important for understanding the mechanism of magnetic reconnection. The first feature suggests that the structure of current layer is modified by the plasma density configuration which is controlled by massive ions although the current is carried predominantly by the electrons. The second feature implies that the electron frozen-in condition is broken mainly by the electron inertia effect in steady magnetic reconnection.

The spatial configurations of five physical quantities at $\omega_{ce0}t = 980$ are plotted in Figure 4, where the blue and red colors respectively denote the low and high values and the different normalization values are used for each panel (hereafter). The top panel shows the magnetic field configuration in the steady state where an X point lies at the center. The electron out-of-plane flow velocity u_{ez}, which is higher than the ion out-of-plane flow velocity $|u_{iz}|$ almost everywhere, forms a sharp peak around the neutral line with the half-width about δ_e (see the second panel). The ion out-of-plane flow exhibits a two-peak structure where the peak-to-peak distance is about $2\rho_i$ in the region of $|x| < 0.3x_b$ and slightly wider outside (the third panel). It is interesting to note in the fourth panel that a low density channel is formed along the x-axis in the electron number density configuration. The channel width, which is defined as the peak-to-peak distances, is $2\rho_i$. The fact that the electron number density is of ion orbit scale ρ_i implies that the density is controlled by ion motion through the electrostatic interaction between ions and electrons. Similarly, the ion temperature T_i is strongly peaked on the x-axis with the width $2\rho_i$ (not shown here). It is noteworthy from the bottom panel that due to the modulation of the plasma density the current layer has the width of about $2\rho_i$ around the X point but its maxima are on both sides of the system along the x-axis.

By examining whether the frozen-in constraint, $\mathbf{E} + \mathbf{u_s} \times \mathbf{B} \approx \mathbf{0}$, holds, we find that the ion motion decouples from the magnetic field within a region of the ion skin depth $c/\omega_{pi} \approx 40\Delta y \approx 2\rho_i$ from the x-axis, while the electrons remain frozen in the magnetic field until they enter a region of scale δ_e.

The above observation of fluid quantities suggests that the dissipation region in the steady phase is of a two-scale structure underlying the quite different characteristics scales of electron dynamics and ion dynamics. The inner electron dissipation region is $2\delta_e$ wide and $2 \times 0.4x_b$ ($\approx 2x_d$) long. The ion dissipation region is $2c/\omega_{pi}$ ($\simeq 4\rho_i$) wide and the length is of the order of system length $2x_b$. In other words, the ions are unmagnetized in the whole downstream in the present open model. Ions decouple from magnetic field within a scale length c/ω_{pi} due to the inertia effect, but the ion meandering motion plays an important role in ion dynamics, which characterizes the spatial structures of ion quantities with the scale ρ_i.

The features of reconnection in the growing phase coincides with that of the previous periodic simulations[10,11], which is not the focus of our attention. After reconnection field saturates, the system tends to a steady state and the current layer width relaxes to a scale of the ion meandering orbit size ρ_i from the electron skin depth δ_e. This result clearly differs from the previous work of non-driven reconnection in a closed system[27], in which the current width is scaled by electron skin depth. The difference probably comes from the models used. In the recent MRX experiment[7], the current layer width is found to be about $0.4c/\omega_{pi}$. This result is in good agreement with our simula-

tion in which $d_{jz} \approx \rho_i \approx 0.5c/\omega_{pi}$.

Intermittent phenomena

It is shown in Table I that intermittent phenomena take place when $x_d/x_b = 0.83$. Figure 5 plots the

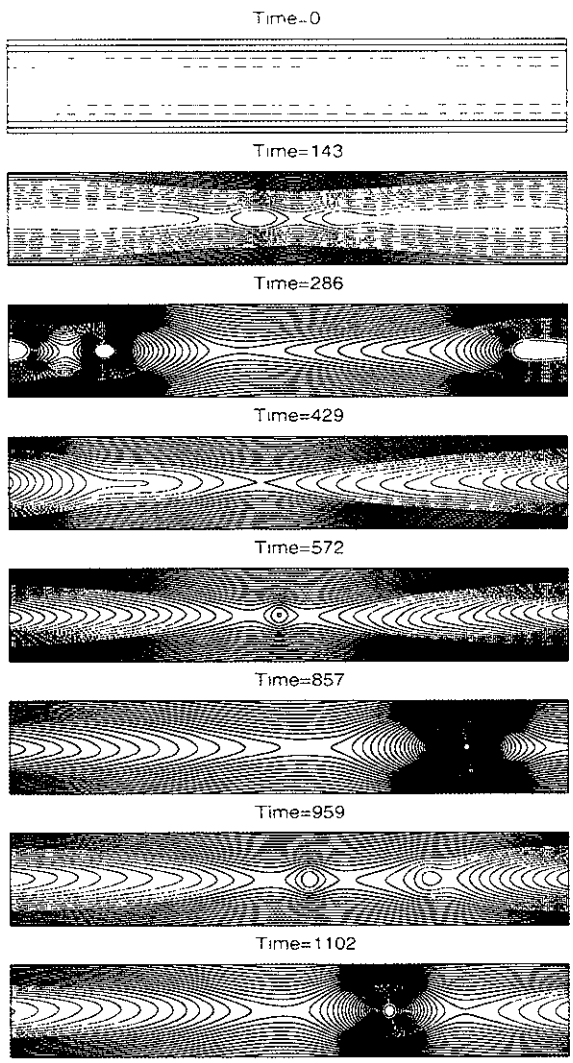

Figure 5: The temporal evolution of magnetic field configuration for Run 3.

temporal evolution of the magnetic field for Run 3. After $\omega_{ce0}t = 550$, magnetic islands frequently turn out from the center, grow up and move out of the system. Figure 5 points out that the system dose not relax toward a steady state, but evolves in an intermittent way because of the frequent generation of magnetic islands. Let us consider why magnetic reconnection evolves in an intermittent way or what mechanism controls the growth of magnetic islands. Figure 6 shows (a) the evolution of the reconnection electric field E_r and (b) those of three spatial scales d_{jz}, ρ_i and ρ_e at the main X point for Run 3. In the saturation phase, the reconnection electric field oscillates around the value of the external driving field E_0 with a larger amplitude compared with Run 1. The fluctuation amplitude increases with x_d for a fixed E_0. One can find that there is a correlation between the growth of islands and the behaviors of these quantities. When an island is produced at the central region (for example, at $\omega_{ce0}t = 550$ and 920), $|E_r|$ is minimum. As the island evolves, the width of current layer at the main X point decreases below ρ_i and $|E_r|$ evolves toward a maximum. When the island is far away the center, d_{jz} return to ρ_i.

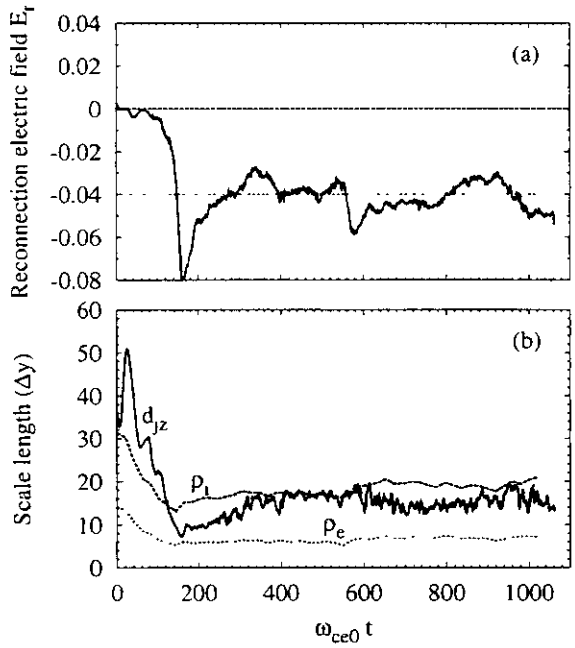

Figure 6: The time histories of (a) reconnection electric field E_r and (b) three spatial scales d_{jz}, ρ_i and ρ_e at the main X point for Run 3.

Figure 7 shows the spatial configurations of the current $-j_z$, the electron flow velocity u_{ez}, the ion flow velocity $-u_{iz}$ and the electron number density at $\omega_{ce0}t = 940$ and 980 when the third island is being formed and growing up, respectively. Figure 7 reveals the following fives facts. First, when the island is formed, the current layer becomes narrower and longer compared with Run 1. Second, the electric current maintaining the island comes mainly from the contribution of electrons rather than ions because $|u_{ez}|$ is much higher than $|u_{iz}|$ in the island. Third, small island structure appears originally in the profile of u_{ez}, which may trigger an instability. Fourth, the island growth requires electric current increases in it. Comparing the quantities at two times, we can find that as time goes on the electron density increases while

the electron velocity decreases at the center of th island. The density increase is caused by the electron trapping inside the island. Therefore, the electric current needed for the growth of the island is supplied by increasing the electron number density. Fifth, two islands are excited by the locally enhanced current density, but only the one near the center can grow up. These characters lead us to the conclusion that the island excitation in the intermittent behavior for $x_d/x_b = 0.83$ is related to the electron dynamics.

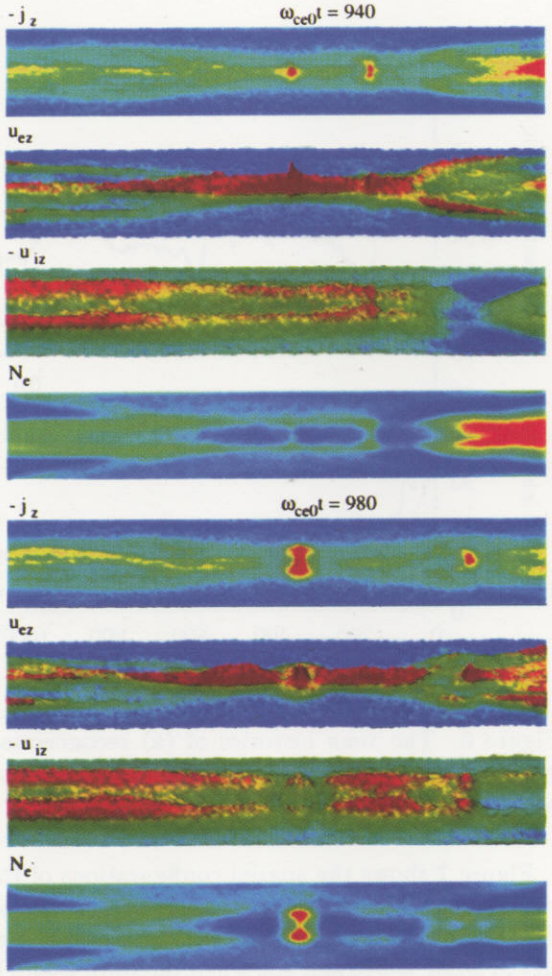

Figure 7: The spatial structures of the out-of-plane current density $-j_z$, the electron flow velocity u_{ez}, the ion flow velocity $-u_{iz}$ and the electron number density N_e at times $\omega_{ce0}t = 940$ (top four panels) and 980 (bottom four panels) for Run 3 where u_{ez}, $-u_{iz}$ and $-j_z$ are perspectively plotted.

Influence of driving electric field

In order to understand why the behavior of driven reconnection is dependent on the nonuniformity scale x_d but independent of the driving field strength E_0, we examine their influence on the spatial structure of the current layer and magnetic field based on the simulation results. The dependences of the electron number density, the electron out-of-plane flow velocity, and the half-width of the current profile on the scale x_d at the X point are plotted in Figure 8. It can be seen that, as x_d increases, the electron density increases and the current layer becomes narrow, while the electron flow velocity remains almost constant. This phenomenon can be explained as follows. As x_d increases, the curvature of input magnetic field lines and the divergency of the corresponding input plasma inflow decrease. Consequently, the particle number entering the reconnection region increases and the current layer is more strongly compressed with x_d, which leads to the density increase. In other words, the parameter x_d controls the density profile of the current layer through the ion dynamics.

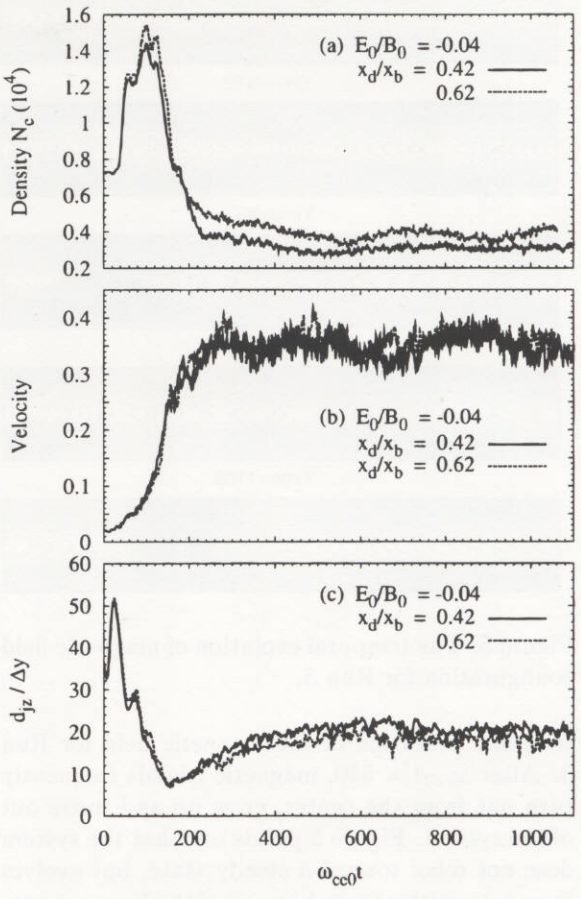

Figure 8: The histories of (a) electron number density N_e, (b) electron flow velocity u_{ez} and (c) half-width of current layer at the X point for Runs 1 and 2.

Figure 9 shows the dependences of the electron

number density, the electron out-of-plane flow velocity, and the half-width of the current profile on the strength E_0. As E_0 increases, both electron number density and electron out-of-plane flow velocity increase and the current layer becomes narrow. The density increase is deeply related to the fact that the input plasma mass flux increases in proportion to E_0. The electron velocity increase is due to the electron acceleration by the electric field E_z.

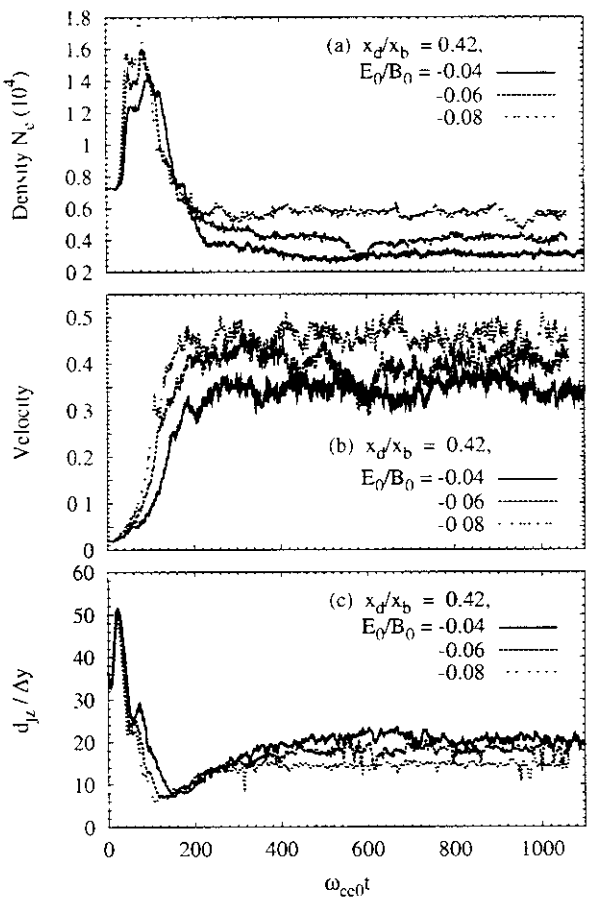

Figure 9: Same as Fig. 8 for Runs 1, 4 and 7.

Let us examine the global structure of current layer and the corresponding magnetic field. Figure 10 plots the dependences of magnetic separatrix structures on x_d (top) and E_0 (bottom). The shape of current layer becomes narrow and flat, and thus the angle between separatrices reduces distinctively, as x_d increases. However, the separatrix shape is insensitive to E_0. When E_0 increases, because the current layer is similarly compressed, its aspect ratio is not changed. This fact implies that the separatrix (or current layer) shape is the key to understand the intermittent behavior of driven reconnection. That is, the flat separatrix facilitates the excitation of magnetic island. On the other hand, because the global shape of magnetic separatrices and so the angle between the separatrices remain almost unchanged when the strength E_0 changes, the reconnection behavior is insensitive to the change in the strength E_0.

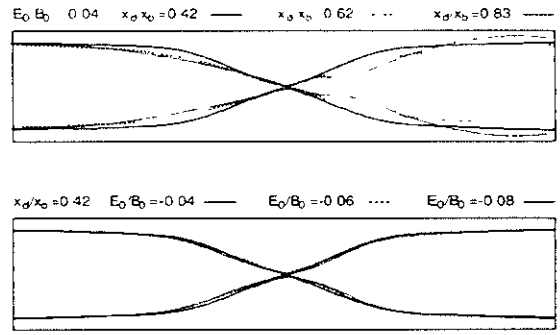

Figure 10: Comparison between the separatrix shapes for different x_d (top panel) and different E_0 (bottom panel).

It is concluded that in a large x_d case collisionless reconnection reveals an intermittent behavior through the frequent generation of magnetic islands because of electron dynamics.

IV CONCLUSION

We have presented first results of particle simulation of collisionless driven reconnection in an open system. In order to study the long time scale evolution of collisionless driven reconnection, we have developed a new simulation model for an open system. In this model, a free physical condition is used at the downstream boundary, across which particles can freely go in and out. At the upstream boundary the driving condition can be uniquely determined by an out-of-plane electric field which is described by two key parameters, the strength E_0 and the early non-uniformity scale x_d.

The evolution of collisionless driven reconnection depends strongly on the external driving electric field. The strength E_0 controls the reconnection rate, while the scale x_d controls the current layer shape and thus the magnetic field configuration. It is found that there are two regimes in the long time scale behavior of collisionless reconnection which is mainly controlled by the scale x_d in our simulation parameter range, i.e., steady regime and intermittent regime. In a small x_d case the system evolves toward a steady regime in which steady reconnection is realized and thus the global field topology remains unchanged. On the other hand, in a large x_d case the system evolves into an intermittent regime in which magnetic islands are frequently excited near the center of the current

sheet.

We investigated the physical features of the steady reconnection. The reconnection rate in the steady regime is mainly controlled by the strength of the driving electric field E_0. The dissipation region has two-scale structure corresponding to both the electron dynamics and the ion dynamics. The electron dissipation region is dominated by an electron inertia effect which controls the electron flow velocity. The ion inertia effect is responsible for breaking of the frozen-in constraint for ions, while the ion meandering motion plays an important role in the spatial structures of plasma density, ion flow velocity and ion temperature. Although the current is predominantly carried by electrons, the current layer has the half-width of the ion scale ρ_i because of modulation of the density profile which is exclusively controlled by the massive ion motion. Thus the global dynamic process of steady magnetic reconnection is dominantly controlled by ion dynamics. The current layer width presented in this paper is in good agreement with the result of recent MRX experiment[7].

In the intermittent regime, the island excitation is related to the electron dynamics. The seed island is triggered by the perturbation of electron velocity near the original X point. This island grows up by increasing the electric current through the electron trapping in it. To shed light on the mechanism in the intermittent regime, the effect of the driving parameters E_0 and x_d on the current layer structure and the magnetic field configuration in the regime of steady reconnection has been explored. As E_0 increases, the current layer is similarly compressed, and thus the corresponding magnetic field configuration is almost unchanged. On the contrary, as x_d increases, the current layer becomes narrow and flat in shape so that the angle between the separatrices decreases. The change of the spatial structure is the cause for the island excitation which leads reconnection to the intermittent regime.

ACKNOWLEDGMENTS

Numerical computations in this study is performed on the NIFS MISSION System (Grand Man-Machine Interactive System for Simulation).

References

[1] K. Schindler, J. Geophys. Res. 79, 2803 (1974).

[2] V. M. Vasyliunas, Rev. Geophys. 13, 303 (1975).

[3] A. A. Galeev, in Basic Plasma Physics, edited by A. A. Galeev and R. N. Sudan (North-Holland, New York, 1984), Vol. 2, p. 305.

[4] H. P. Furth, J. Killeen, and M. N. Rosenbluth, Phys. Fluids 6, 459 (1963).

[5] J. F. Drake and Y. C. Lee, Phys. Fluids 20, 1341 (1977).

[6] M. Yamada, F. W. Perkins, A. K. MacAulay, Y. Ono, and M. Katsurai, Phys. Fluids B3, 239 (1991).

[7] M. Yamada, H. Ji, S. Hsu, T. Carter, R. Kulsrud and F. Trintchouk, Phys. Plasmas 7, 1781 (2000).

[8] M. Ottaviani and F. Porcelli, Phys. Rev. Lett. 71, 3802 (1993).

[9] D. Biskamp, E. Schwarz and J. F. Drake, Phys. Rev. Lett. 75, 3850 (1995).

[10] R. Horiuchi and T. Sato, Phys. Plasmas 1, 3587 (1994).

[11] R. Horiuchi and T. Sato, Phys. Plasmas 4, 277 (1997).

[12] H. J. Cai and L. C. Lee, Phys. Plasmas 4, 509 (1997).

[13] M. Hesse, K. Schindler, J. Birn and M. Kuznetsova, Phys. Plasmas 6, 1781 (1999).

[14] G. Laval, R. Pellat, and M. Vuillemin, Plasma Physics and Controlled Fusion Research (International Atomic Energy Agency, Vienna, 1966), Vol. II, p. 259.

[15] B. Coppi, G. Laval and R. Pellat, Phys. Rev. Lett. 16, 1207 (1966).

[16] X. Wang and A. Bhatacharjee, J. Geophys. Res. 98, 19419 (1993).

[17] I. Katanuma and T. Kamimura, Phys. Fluids 23, 2500 (1980).

[18] W. Zwingmann, J. Wallance, K. Schindler, and J. Birn, J. Geophys. Res. 95, 20877 (1990).

[19] P. L. Pritchett, F. V. Coroniti, R. Pellat, and H. Karimabadi, J. Geophys. Res. 96, 11523 (1991).

[20] T. Sato and T. Hayashi, Phys. Fluids 22, 1189 (1979).

[21] T. S. Hahm and R. M. Kulsrud, Phys. Fluids 28, 2412 (1985).

[22] X. Wang and A. Bhattacharjee, Phys. Fluids B4, 1795 (1992)

[23] X. Wang, Z. W. Ma and A. Bhattacharjee, Phys. Plasmas 3, 2129 (1996)

[24] X. Wang, A. Bhattacharjee and Z. W. Ma, J. Geophys. Res. 105, 27633 (2000).

[25] H. Kitabata, T. Hayashi, T. Sato, R. Horiuchi, K. Watanabe, A. Kageyama, T. H. Watanabe, Y. Todo, and H. Takamaru, J. Phys. Soc. Japan, 65, 3208 (1996).

[26] H. Amo, T. Sato, A. Kageyama, K. Watanabe, R. Horiuchi, T. Hayashi, Y. Todo, T. H. Watanabe, and H. Takamaru, Phys. Rev., E51, 3838 (1995)

[27] M. A. Shay, J. F. Drake and B. N. Rogers, Geophys. Res. Lett. 26, 2163 (1999).

Recent Issues of NIFS Series

NIFS-669 K. Mima, M.S. Jovanovic, Y. Sentoku, Z-M. Sheng, M.M. Skoric and T. Sato,
Stimulated Photon Cascade and Condensate in Relativistic Laser plasma Interaction, Nov. 2000

NIFS-670 I. Hadzievski, M.M. Skoric and T. Sato,
On Origin and Dynamics of the Discrete NLS Equation, Nov. 2000

NIFS-671 K. Ohkubo, S. Kubo, H. Idei, T. Shimozuma, Y. Yoshimura, F. Leuterer, M. Sato and Y. Takita,
Analysis of Oversized Sliding Waveguide by Mode Matching and Multi-Mode Network Theory, Dec. 2000

NIFS-672 C. Das, S. Kida and S. Goto,
Overall Self-Similar Decay of Two-Dimensional Turbulence, Dec. 2000

NIFS-673 L.A. Bureyeva, T. Kato, V.S. Lisitsa and C. Namba,
Quasiclassical Representation of Autoionization Decay Rates in Parabolic Coordinates, Dec. 2000

NIFS-674 L.A. Bureyeva, V.S. Lisitsa and C. Namba,
Radiative Cascade Due to Dielectronic Recombination, Dec. 2000

NIFS-675 M.F.Heyn, S.V. Kasilov, W. Kernbichler, K. Matsuoka, V.V. Nemov, S. Okamura, O.S. Pavlichenko,
Configurational Effects on Low Collision Plasma Confinement in CHS Heliotron/Torsatron, Jan. 2001

NIFS-676 K. Itoh,
A Prospect at 11th International Toki Conference - Plasma physics quo vadis?, Jan. 2001

NIFS-677 S. Satake, H. Sugama, M. Okamoto and M. Wakatani,
Classification of Particle Orbits near the Magnetic Axis in a Tokamak by Using Constants of Motion, Jan. 2001

NIFS-678 M. Tanaka and A. Yu. Grosberg,
Giant Charge Inversion of a Macroion Due to Multivalent Counterions and Monovalent Coions: Molecular Dynamics Studyn, Jan. 2001

NIFS-679 K. Akaishi, M. Nakasuga, H. Suzuki, M. Iima, N. Suzuki, A. Komori, O. Motojima and Vacuum Engineering Group,
Simulation by a Diffusion Model for the Variation of Hydrogen Pressure with Time between Hydrogen Discharge Shots in LHD, Feb. 2001

NIFS-680 A. Yoshizawa, N. Yokoi, S. Nisizima, S.-I. Itoh and K. Itoh,
Variational Approach to a Turbulent Swirling Pipe Flow with the Aid of Helicity, Feb. 2001

NIFS-681 Alexander A. Shishkin,
Estafette of Drift Resonances, Stochasticity and Control of Particle Motion in a Toroidal Magnetic Trap, Feb. 2001

NIFS-682 H. Momota and G.H. Miley,
Virtual Cathode in a Spherical Inertial Electrostatic Confinement Device, Feb. 2001

NIFS-683 K. Saito, R. Kumazawa, T. Mutoh, T. Seki, T. Watari, Y. Torii, D.A. Hartmann, Y. Zhao, A. Fukuyama, F. Shimpo, G. Nomura, M. Yokota, M. Sasao, M. Isobe, M. Osakabe, T. Ozaki, K. Narihara, Y. Nagayama, S. Inagaki, K. Itoh, S. Morita, A.V. Krasilnikov, K. Ohkubo, M. Sato, S. Kubo, T. Shimozuma, H. Idei, Y. Yoshimura, O. Kaneko, Y. Takeiri, Y. Oka, K. Tsumori, K. Ikeda, A. Komori, H. Yamada, H. Funaba, K.Y. Watanabe, S. Sakakibara, M. Shoji, R. Sakamoto, J. Miyazawa, K. Tanaka, B.J. Peterson, N. Ashikawa, S. Murakami, T. Minami, S. Ohakachi, S. Yamamoto, S. Kado, H. Sasao, H. Suzuki, K. Kawahata, P. deVries, M. Emoto, H. Nakanishi, T. Kobuchi, N. Inoue, N. Ohyabu, Y. Nakamura, S. Masuzaki, S. Muto, K. Sato, T. Morisaki, M. Yokoyama, T. Watanabe, M. Goto, I. Yamada, K. Ida, T. Tokuzawa, , N. Noda, S. Yamaguchi, K. Akaishi, A. Sagara, K. Toi, K. Nishimura, K. Yamazaki, S. Sudo, Y. Hamada, O. Motojima, M. Fujiwara,
Ion and Electron Heating in ICRF Heating Experiments on LHD, Mar. 2001

NIFS-684 S. Kida and S. Goto,
Line Statistics Stretching Rate of Passive Lines in Turbulence, Mar. 2001

NIFS-685 R. Tanaka, T. Nakamura and T. Yabe,
Exactly Conservative Semi-Lagrangian Scheme (CIP-CSL) in One-Dimension, Mar. 2001

NIFS-686 S. Toda and K. Itoh,
Analysis of Structure and Transition of Radial Electric Field in Helical Systems, Mar. 2001

NIFS-687 T. Kuroda and H. Sugama,
Effects of Multiple-Helicity Fields on Ion Temperature Gradient Modes, Apr. 2001

NIFS-688 M. Tanaka,
The Origins of Elctrical Resistivity in Magnetic Reconnection: Studies by 2D and 3D Macro Particle Simulations, Apr. 2001

NIFS-689 A. Maluckov, N. Nakajima, M. Okamoto, S. Murakami and R. Kanno,
Statistical Properties of the Neoclassical Radial Diffusion in a Tokamak Equilibrium, Apr. 2001

NIFS-690 Y. Matsumoto, T. Nagaura, Y. Itoh, S-I. Oikawa and T. Watanabe,
LHD Type Proton-Boron Reactor and the Control of its Peripheral Potential Structure, Apr. 2001

NIFS-691 A. Yoshizawa, S.-I. Itoh, K. Itoh and N. Yokoi,
Turbulence Theories and Modelling of Fluids and Plasmas, Apr. 2001

NIFS-692 K. Ichiguchi, T. Nishimura, N. Nakajima, M. Okamoto, S.-i. Oikawa, M. Itagaki,
Effects of Net Toroidal Current Profile on Mercier Criterion in Heliotron Plasma, Apr. 2001

NIFS-693 W. Pei, R. Horiuchi and T. Sato,
Long Time Scale Evolution of Collisionless Driven Reconnection in a Two-Dimensional Open System, Apr. 2001